

# Vacuum Stability, Perturbativity, EWPD and Higgs-to-diphoton in Type II Seesaw

Eung Jin Chun, Hyun Min Lee, and Pankaj Sharma  
Korea Institute for Advanced Study, Seoul 130-722, Korea

We study constraints from perturbativity and vacuum stability as well as the EWPD in the type II seesaw model. As a result, we can put stringent limits on the Higgs triplet couplings depending on the cut-off scale. The EWPD tightly constrain the Higgs triplet mass splitting to be smaller than about 40 GeV. Analyzing the Higgs-to-diphoton rate in the allowed parameter region, we show how much it can deviate from the Standard Model prediction for specific parameter points.

## I. INTRODUCTION

The discovery of the Higgs boson at around 125 GeV [1] opened a new era toward the Higgs precision test. It is essential for the LHC and future experiments to determine how precisely the Higgs candidate follows the very prediction of the Standard Model (SM), as new physics might enter here to modify the SM Higgs property in various ways. One of the motivations for new physics beyond the SM comes from the smallness of neutrino masses whose origin can be attributed to a new particle coupling to the lepton doublets of the SM.

In this paper [2], we consider the type II seesaw mechanism which introduces a Higgs triplet whose vacuum expectation value (VEV) generates the neutrino masses and mixing [3]. The Higgs sector of the type II seesaw contains four more bosons,  $H^{++}$ ,  $H^+$  and  $H^0/A^0$ , in addition to the SM Higgs boson,  $h$ . While the standard Higgs doublet generates the quark and charged lepton masses, the Higgs triplet couples only to the lepton doublets generating the neutrino masses. This mechanism leads to a peculiar prediction of a same-sign dilepton resonance,  $H^{++} \rightarrow l_\alpha^+ l_\beta^+$ , which is being searched at the LHC [4]. As the Higgs triplet Yukawa matrix is proportional to the neutrino mass matrix, the observation of the flavor structure of the same-sign dilepton final states allows us to determine the neutrino mass pattern at colliders [5].

Other interesting features of the type II seesaw come from the Higgs boson sector. Considering the perturbativity and absolute vacuum stability conditions up to the Planck scale, the perturbativity keeps a triplet self coupling, denoted by  $\lambda_2$ , smaller than 0.25 and then vacuum stability requires all the other couplings to be smaller than 0.5. If a lower instability scale is taken, such a stringent limit can of course be relaxed, but not too much. Another important constraint can be deduced from the electroweak precision data (EWPD) [6]. Note that one of the couplings between the Higgs triplet and doublet, denoted by  $\lambda_5$ , induces mass splitting  $\Delta M$  among the triplet components [5]. The EWPD turn out to put a strong limit of  $|\Delta M| \lesssim 40$  GeV allowing only a narrow range of  $\lambda_5$  depending on the Higgs triplet mass when the triplet VEV is taken to be tiny enough so that its tree-level contribution to  $\Delta\rho$  is neglected.

As noted in [7–9], the SM Higgs boson decay  $h \rightarrow \gamma\gamma$  can be significantly modified through one-loop diagrams involving the charged Higgs bosons, in particular,  $H^{++}$ , if quartic couplings mixing with the SM Higgs are large and the triplet mass is small. The precise measurement of the diphoton rate will place an important restriction on the type II seesaw model. In our analysis, we show how much the  $h \rightarrow \gamma\gamma$  rate can deviate from the SM prediction after restricting ourselves to the model parameter space allowed by the perturbativity and vacuum stability conditions as well as the EWPD constraint, which has not been considered properly in the previous studies.

## II. HIGGS COUPLINGS IN TYPE II SEESAW

When the Higgs sector of the Standard Model is extended with a  $Y = 2$   $SU(2)_L$  scalar triplet  $\Delta$  in addition to a SM-Higgs doublet  $\Phi$ , the gauge-invariant Lagrangian is written as

$$\mathcal{L} = (D_\mu \Phi)^\dagger (D^\mu \Phi) + \text{Tr} (D_\mu \Delta)^\dagger (D^\mu \Delta) - \mathcal{L}_Y - V(\Phi, \Delta)$$

where the leptonic part of the Lagrangian required to generate neutrino masses is

$$\mathcal{L}_Y = f_{\alpha\beta} L_\alpha^T C i \tau_2 \Delta L_\beta + \text{H.c.} \quad (1)$$

and the scalar potential is

$$\begin{aligned}
V(\Phi, \Delta) = & m^2 \Phi^\dagger \Phi + \lambda_1 (\Phi^\dagger \Phi)^2 + M^2 \text{Tr}(\Delta^\dagger \Delta) \\
& + \lambda_2 [\text{Tr}(\Delta^\dagger \Delta)]^2 + 2\lambda_3 \text{Det}(\Delta^\dagger \Delta) + \lambda_4 (\Phi^\dagger \Phi) \text{Tr}(\Delta^\dagger \Delta) \\
& + \lambda_5 (\Phi^\dagger \tau_i \Phi) \text{Tr}(\Delta^\dagger \tau_i \Delta) + \left[ \frac{1}{\sqrt{2}} \mu (\Phi^T i \tau_2 \Delta^\dagger \Phi) + \text{H.c.} \right].
\end{aligned} \tag{2}$$

Here used is the  $2 \times 2$  matrix representation of  $\Delta$ :

$$\Delta = \begin{pmatrix} \Delta^+/\sqrt{2} & \Delta^{++} \\ \Delta^0 & -\Delta^+/\sqrt{2} \end{pmatrix}. \tag{3}$$

Upon the electroweak symmetry breaking with  $\langle \Phi^0 \rangle = v_0/\sqrt{2}$ , the  $\mu$  term in Eq. (2) gives rise to the vacuum expectation value of the triplet  $\langle \Delta^0 \rangle = v_\Delta/\sqrt{2}$  where  $v_\Delta \approx \mu v_0^2/\sqrt{2}M^2$ . We will assume  $\mu$  is real positive without loss of generality. From the leptonic Yukawa coupling (1), one can get the neutrino mass matrix

$$M_{\alpha\beta}^\nu = f_{\alpha\beta} \xi v_0, \tag{4}$$

where  $\xi \equiv v_\Delta/v_0$ . The observed neutrino mass of order 0.1 eV requires  $|f_{\alpha\beta} \xi| \sim 10^{-12}$ . Considering this relation, we will assume  $|f_{\alpha\beta}| \ll 1$  and  $|\xi| \ll 1$  throughout this work. Let us remind that the measurement of  $\rho \equiv M_W^2/(M_Z^2 c_W^2) \approx 1$  puts the bound  $\xi \lesssim 10^{-2}$ . We will work in the region of  $|\xi| \ll 10^{-2}$  for our analysis.

After the electroweak symmetry breaking, there are five physical massive bosons denoted by  $H^{\pm\pm}$ ,  $H^\pm$ ,  $H^0$ ,  $A^0$ ,  $h^0$ . Under the condition of  $|\xi| \ll 1$ , the first five states are mainly from the triplet scalar and the last from the doublet scalar. For the neutral pseudoscalar and charged scalar parts,

$$\begin{aligned}
\phi_I^0 &= G^0 - 2\xi A^0, & \phi^+ &= G^+ + \sqrt{2}\xi H^+ \\
\Delta_I^0 &= A^0 + 2\xi G^0, & \Delta^+ &= H^+ - \sqrt{2}\xi G^+
\end{aligned} \tag{5}$$

where  $G^0$  and  $G^+$  are the Goldstone modes, and for the neutral scalar part,

$$\begin{aligned}
\phi_R^0 &= h^0 - a\xi H^0, \\
\Delta_R^0 &= H^0 + a\xi h^0
\end{aligned} \tag{6}$$

where  $a = 2 + (4\lambda_1 - \lambda_4 - \lambda_5)v_0^2/(M_{H^0}^2 - M_{h^0}^2)$ . The masses of the Higgs bosons essentially from the triplet are

$$\begin{aligned}
M_{H^{\pm\pm}}^2 &= M^2 + \frac{\lambda_4 - \lambda_5}{2} v_0^2 \\
M_{H^\pm}^2 &= M_{H^{\pm\pm}}^2 + \frac{\lambda_5}{2} v_0^2 \\
M_{H^0, A^0}^2 &= M_{H^{\pm\pm}}^2 + \lambda_5 v_0^2,
\end{aligned} \tag{7}$$

neglecting small contributions from  $v_\Delta$ . The mass of  $h^0$  is given by  $m_{h^0}^2 = 2\lambda_1 v_0^2$  as usual.

Eq. (7) tells us that the mass splitting,  $\Delta M \equiv M_{H^\pm} - M_{H^{\pm\pm}}$ , is driven by the coupling  $\lambda_5$  which affects also the EWPD and the Higgs-to-diphoton rate. Recall that depending upon the sign of the coupling  $\lambda_5$ , there are two mass hierarchies among the triplet components:  $M_{H^{\pm\pm}} > M_{H^\pm} > M_{H^0, A^0}$  for  $\lambda_5 < 0$ ; or  $M_{H^{\pm\pm}} < M_{H^\pm} < M_{H^0, A^0}$  for  $\lambda_5 > 0$  [5]. The charged Higgs boson as light as 100 GeV ( $M_{H^{\pm\pm}}$  or  $M_{H^\pm} = 100$  GeV) can evade the CMS search if the decay channels of  $H^{\pm\pm} \rightarrow H^\pm W^*$  and  $H^\pm \rightarrow H^0/A^0 W^*$  are the dominant modes allowed by a sizable  $\lambda_5$  in the first case, or if  $H^{\pm\pm}$  decays dominantly to  $W^\pm W^\pm$  with  $|\xi| \gg |f_{ij}|$  in the second case.

### III. VACUUM STABILITY AND PERTURBATIVITY

The scalar potential (2) contains seven free parameters:  $\lambda_i$  ( $i = 1 \dots 5$ ),  $v_\Delta$  and  $M_{H^{\pm\pm}}$ . Rather stringent constraints on these parameters can be readily obtained by the theoretical requirements of perturbativity and

vacuum stability. A detailed study of the scalar potential has been performed in [11]. The vacuum stability conditions on the scalar couplings  $\lambda_i$  are as follows:

$$\begin{aligned} \lambda_1 > 0, \quad \lambda_2 > 0, \quad \lambda_2 + \frac{1}{2}\lambda_3 > 0 \\ \lambda_4 \pm \lambda_5 + 2\sqrt{\lambda_1\lambda_2} > 0, \quad \lambda_4 \pm \lambda_5 + 2\sqrt{\lambda_1(\lambda_2 + \frac{1}{2}\lambda_3)} > 0. \end{aligned} \quad (8)$$

Apart from these conditions, we will put the perturbativity conditions:  $|\lambda_i| \leq \sqrt{4\pi}$ .

We will take the absolute stability condition that all these constraints must remain true up to the scale where the theory is supposed to be valid. Henceforth, we study the renormalization group (RG) evolution of these scalar couplings ( $\lambda_i$ 's), EW-gauge couplings  $g_2$ ,  $g'$ , strong coupling  $g_3$  and top-Yukawa coupling  $y_t$  up to the cut-off scale at the one-loop level. The RG evolution of the type II seesaw model has been studied in [12].

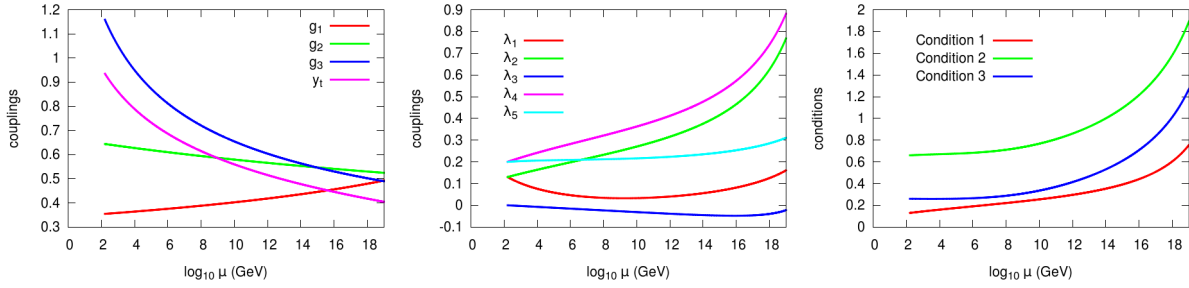


FIG. 1: RG evolution of couplings and vacuum stability conditions.

In Fig. 1, we show an example of the RG running of the couplings which maintain the perturbativity and vacuum stability up to the Planck scale. In the rightmost panel, the three vacuum stability conditions; (1)  $\lambda_2 + \frac{1}{2}\lambda_3 > 0$ , (2)  $\lambda_4 - \lambda_5 + 2\sqrt{\lambda_1\lambda_2} > 0$ , and (3)  $\lambda_4 - \lambda_5 + 2\sqrt{\lambda_1(\lambda_2 + \frac{1}{2}\lambda_3)} > 0$  are presented. Note that the Higgs doublet self-coupling  $\lambda_1$  decreases initially due to the top Yukawa coupling as in the SM, but it turns around to increase at a certain point with the aid of other increasing couplings. For our numerical analysis, we use  $M_t = 173$  GeV,  $m_t(M_t) = 164$  GeV,  $m_h = 125$  GeV and thus  $\lambda_1(M_t) = m_h^2/2v_0^2 = 0.129$  and  $y_t(M_t) = \sqrt{2}m_t/v_0 = 0.938$ .

#### IV. CONSTRAINTS FROM EWPD

In this section, we study the contributions of the Higgs triplet to the EWPD observables, also known as the oblique parameters. In [13], the contribution of a scalar multiplet of arbitrary weak isospin and weak hypercharge to the  $S$ ,  $T$  and  $U$  parameters has been calculated. We present here the expressions for the specific case of the Higgs triplet model:

$$\begin{aligned} S &= -\frac{1}{3\pi} \ln \frac{m_{+1}^2}{m_{-1}^2} - \frac{2}{\pi} \sum_{T_3=-1}^{+1} (T_3 - Qs_W^2)^2 \xi \left( \frac{m_{T_3}^2}{m_Z^2}, \frac{m_{T_3}^2}{m_Z^2} \right) \\ T &= \frac{1}{16\pi c_W^2 s_W^2} \sum_{T_3=-1}^{+1} (2 - T_3(T_3 - 1)) \eta \left( \frac{m_{T_3}^2}{m_Z^2}, \frac{m_{T_3-1}^2}{m_Z^2} \right) \\ U &= \frac{1}{6\pi} \ln \frac{m_0^4}{m_{+1}^2 m_{-1}^2} + \frac{1}{\pi} \sum_{T_3=-1}^{+1} \left[ 2(T_3 - Qs_W^2)^2 \xi \left( \frac{m_{T_3}^2}{m_Z^2}, \frac{m_{T_3}^2}{m_Z^2} \right) \right. \\ &\quad \left. - (2 - T_3(T_3 - 1)) \xi \left( \frac{m_{T_3}^2}{m_W^2}, \frac{m_{T_3}^2}{m_W^2} \right) \right] \end{aligned} \quad (9)$$

where  $m_{+1,0,-1} = M_{H^{++}, H^+, H^0}$  and the functions  $\xi(x, y)$  and  $\eta(x, y)$  are defined in [13].

Adopting the most recent fit results for the allowed regions of the  $S$ ,  $T$  and  $U$  presented in [14], we use the following values for the SM fit of the oblique parameters:

$$\begin{aligned} S_{\text{best fit}} &= 0.03, & \sigma_S &= 0.10, \\ T_{\text{best fit}} &= 0.05, & \sigma_T &= 0.12, \\ U_{\text{best fit}} &= 0.03, & \sigma_U &= 0.10, \end{aligned} \quad (10)$$

As the  $S$ ,  $T$  and  $U$  are not independent quantities, there is a correlation among these quantities. The correlation coefficients are given by

$$\rho_{ST} = 0.89, \quad \rho_{SU} = -0.54, \quad \rho_{TU} = -0.83. \quad (11)$$

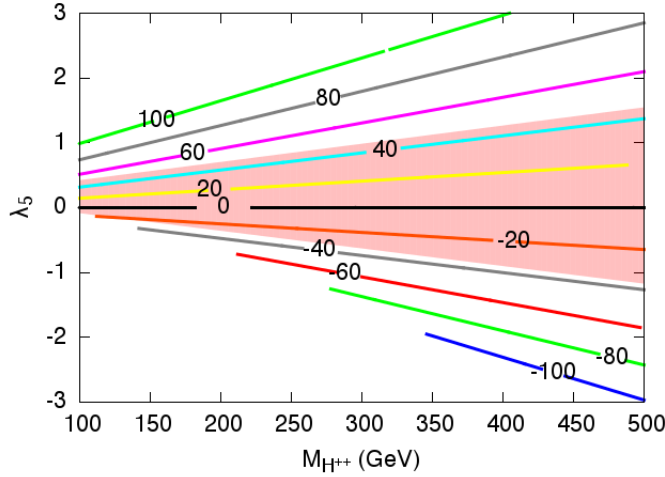


FIG. 2: Allowed parameter space in the  $M_{H^{++}} - \lambda_5$  plane. The contours represent the allowed values of mass splitting,  $\Delta M \equiv M_{H^+} - M_{H^{++}}$ , in the unit of GeV. The shaded band denotes the 99% CL region satisfying the EWP constraint.

In Fig. 2, we show the allowed parameter space in the  $M_{H^{++}} - \lambda_5$  plane consistent with the EWP. The shaded region shows the EWP constraint at 99% CL. The contour lines show the mass splitting,  $\Delta M \equiv M_{H^+} - M_{H^{++}}$ , from which one can see that the mass splitting is tightly constrained to be within  $|\Delta M| \lesssim 40$  GeV independently of the doubly charged Higgs mass.

## V. HIGGS TRIPLET CONTRIBUTION TO $h \rightarrow \gamma\gamma$

Having studied the consistency conditions on the model parameters, we now analyze their impact on the Higgs boson decay to two photons. In the type II seesaw model, the Higgs-to-diphoton decay rate gets a sizable contribution from the charged Higgs bosons,  $H^{++}$  and  $H^+$ , which can lead to a constructive or destructive interference with the SM contribution from the top quark and weak gauge boson. Summing up all the contributions, one gets the following Higgs-to-diphoton rate:

$$\begin{aligned} \Gamma(h \rightarrow \gamma\gamma) &= \frac{G_F \alpha^2 m_h^3}{128 \sqrt{2} \pi^3} \left| \sum_f N_c Q_f^2 g_{ff}^h A_{1/2}^h(x_f) + g_{WW}^h A_1^h(x_W) \right. \\ &\quad \left. + g_{H^+H^-}^h A_0^h(x_{H^+}) + 4g_{H^{++}H^{--}}^h A_0^h(x_{H^{++}}) \right|^2 \end{aligned} \quad (12)$$

where  $x_i = m_h^2/4m_i^2$  and the functions are

$$\begin{aligned} A_{1/2}^h(x) &= 2x^{-2}[x + (x-1)f(x)] \\ A_1^h(x) &= -x^{-2}[2x^2 + 3x + 3(2x-1)f(x)] \\ A_0^h(x) &= -x^{-2}[x - f(x)] \\ \text{where } f(x) &= \begin{cases} \arcsin^2 \sqrt{x} & \text{for } x \leq 1 \\ -\frac{1}{4} \left[ \ln \frac{1+\sqrt{1-x^{-1}}}{1-\sqrt{1-x^{-1}}} - i\pi \right]^2 & \text{for } x > 1 \end{cases} \end{aligned} \quad (13)$$

The Higgs couplings are  $g_{ff}^h = 1$  for the top and  $g_{WW}^h = 1$ , whereas the Higgs triplet couplings are

$$g_{H^+H^+}^h = \frac{\lambda_4}{2} \frac{v_0^2}{M_{H^+}^2}, \quad \text{and} \quad g_{H^{++}H^{++}}^h = \frac{\lambda_4 - \lambda_5}{2} \frac{v_0^2}{M_{H^{++}}^2}. \quad (14)$$

Since the SM contribution amounts to about  $-6.5$  in the amplitude, negative values of  $\lambda_4$  and  $\lambda_4 - \lambda_5$  can make a constructive interference to enhance the diphoton rate. As we will see in the next section, however, the vacuum stability condition strongly disfavors negative  $\lambda_4$  and  $\lambda_4 - \lambda_5$  and allows more parameter region leading to a destructive interference to reduce the diphoton rate.

## VI. RESULTS AND SUMMARY

In this section we perform a numerical analysis to constrain the parameter space of the scalar couplings by considering the conditions of vacuum stability and perturbativity up to the scale where the theory is considered to be valid. We present our results only for the instability scale  $10^{19}$  GeV. We further look for the allowed parameter space combining these with the EWPD and quantify the deviation of the ratio  $R_{\gamma\gamma}$  from the SM value  $R_{\gamma\gamma}^{SM} = 1$ . Figs. 3 summarize our results in the  $\lambda_4$ - $\lambda_5$  plane with different values of  $\lambda_2$  and  $\lambda_3$  for the doubly charged Higgs mass,  $M_{H^{++}} = 100$  GeV (left), 150 GeV (middle) and 200 GeV (right). The contours represent the values of  $R_{\gamma\gamma}$ . The gray (purple) bands denote the 99% (95% CL) region satisfying the EWPD constraints.

We infer from these figures that for negative  $\lambda_3$ , larger values of  $\lambda_2$  are allowed while for positive  $\lambda_3$ , smaller values of  $\lambda_2$  are preferred to satisfy vacuum stability conditions. We observe that a large  $\lambda_2$  tends to squeeze the allowed parameter space in the  $\lambda_4$ - $\lambda_5$  plane. This is due to the fact that a large  $\lambda_2$  violates perturbativity very quickly when we evolve the coupling with RG equations. We find that  $\lambda_3 = 0$  allows for a larger parameter space compared to two extremal values of  $\lambda_3$ . As a result, the enhancement of  $R_{\gamma\gamma}$  is feasible for relatively larger allowed parameter space. The shaded bands in figures denote the allowed region by the EWPD depending on the doubly charged Higgs boson mass. As is obvious, smaller and more positive ranges of  $\lambda_5$  are allowed for smaller values of  $M_{H^{++}}$ . Although the allowed bands of  $\lambda_5$  get smaller for smaller  $M_{H^{++}}$ ,  $R_{\gamma\gamma}$  can be more enhanced in these regions due to the sizable contribution from light charged Higgs bosons, in particular, near  $\lambda_4 = 0$  favored by vacuum stability conditions. Of course, a larger parameter space opens up for a larger positive  $\lambda_4$  for which a destructive interference occurs and thus  $R_{\gamma\gamma}$  can be much smaller than 1. Thus, broad ranges with positive  $\lambda_4$  are strongly disfavored by the current LHC data.

To summarize, we studied the parameter space of the Higgs scalar potential of the type II seesaw model in the light of vacuum stability, perturbativity and EWPD constraints. Then we looked at the possible deviation in the Higgs-to-diphoton rate in the allowed parameter space. The allowed parameter space is found to be very restrictive depending on the choice of the instability scale. Regardless of any choice of instability scale,  $R_{\gamma\gamma}$  becomes smaller than 1 in a larger parameter space, but it can be enhanced by 50%-100% in some limited parameter region. If the deviation of the Higgs-to-diphoton rate turns out to be small with more data at the LHC, only a narrow band around  $\lambda_4 \approx \lambda_5$  will survive for low Higgs triplet mass.

- 
- [1] G. Aad *et al.* [The ATLAS Collaboration], arXiv:1207.7214 [hep-ex]; S. Chatrchyan *et al.* [The CMS Collaboration], arXiv:1207.7235 [hep-ex].
  - [2] E. J. Chun, H. M. Lee and P. Sharma, JHEP **1211**, 106 (2012) [arXiv:1209.1303 [hep-ph]].
  - [3] M. Magg and C. Wetterich, Phys. Lett. B **94** (1980) 61; J. Schechter and J. W. F. Valle, Phys. Rev. D **22** (1980) 2227. T. P. Cheng and L. -F. Li, Phys. Rev. D **22** (1980) 2860; R. N. Mohapatra and G. Senjanovic, Phys. Rev. D **23** (1981) 165.

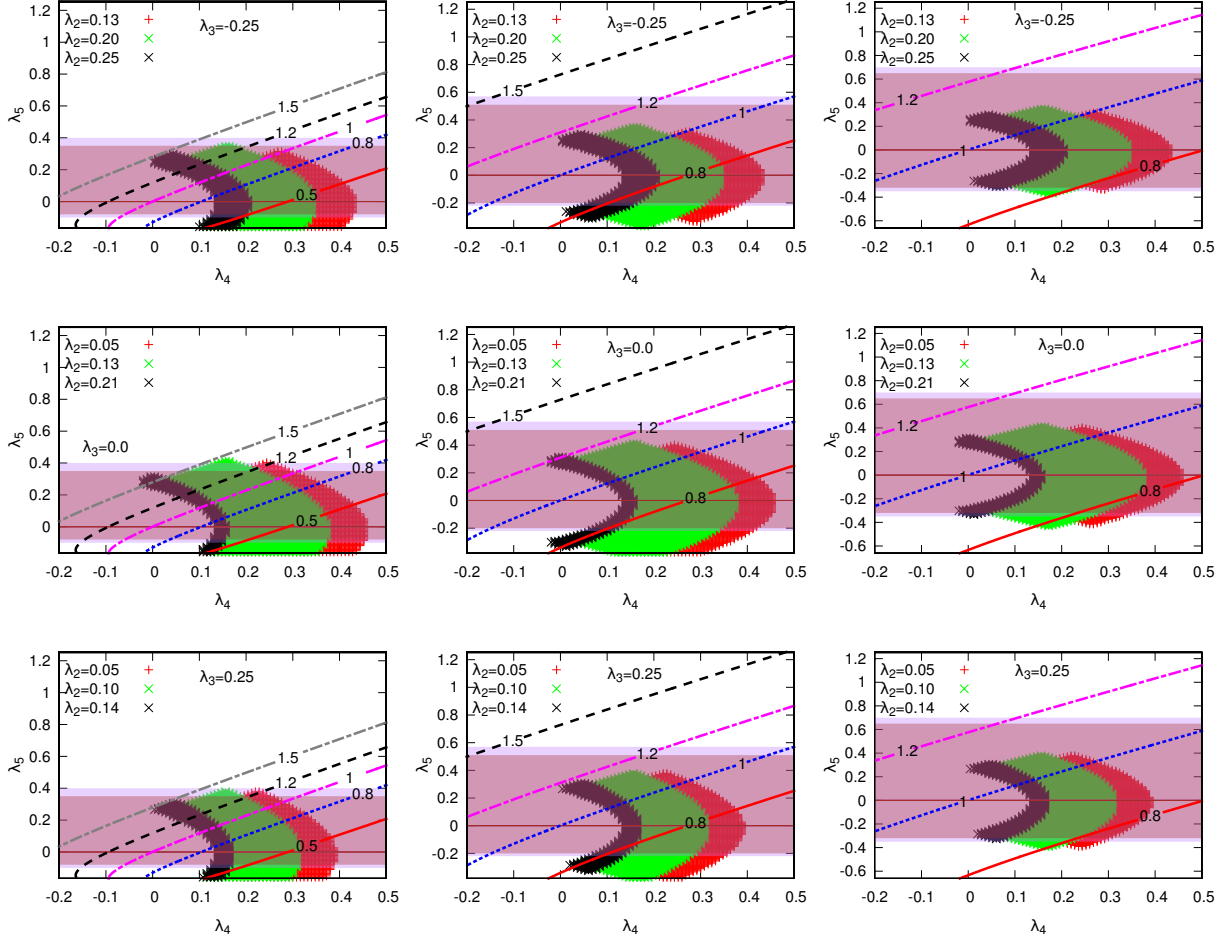


FIG. 3: Allowed parameter space in the  $\lambda_4$ – $\lambda_5$  plane with different values of  $\lambda_2$  and  $\lambda_3$  for the doubly charged Higgs mass,  $M_{H^{++}} = 100$  GeV (left), 150 GeV (middle) and 200 GeV (right). The contours represent the values of  $R_{\gamma\gamma}$ . The gray (purple) bands denote the 99% (95% CL) region satisfying the EWPD constraints. The cut-off scale is assumed to be  $10^{19}$  GeV.

- [4] S. Chatrchyan *et al.* [CMS Collaboration], arXiv:1207.2666 [hep-ex]; G. Aad *et al.* [ATLAS Collaboration], Eur. Phys. J. C **72** (2012) 2244 [arXiv:1210.5070 [hep-ex]].
- [5] E. J. Chun, K. Y. Lee and S. C. Park, Phys. Lett. B **566** (2003) 142 [hep-ph/0304069].
- [6] A. Melfo, M. Nemevsek, F. Nesti, G. Senjanovic and Y. Zhang, Phys. Rev. D **85** (2012) 055018 [arXiv:1108.4416 [hep-ph]].
- [7] A. Arhrib, R. Benbrik, M. Chabab, G. Moultaqa and L. Rahili, JHEP **1204** (2012) 136 [arXiv:1112.5453 [hep-ph]].
- [8] S. Kanemura and K. Yagyu, Phys. Rev. D **85** (2012) 115009 [arXiv:1201.6287 [hep-ph]].
- [9] A. G. Akeroyd and S. Moretti, arXiv:1206.0535 [hep-ph].
- [10] For a detail, see, e.g., E. J. Chun and P. Sharma, JHEP **1208** (2012) 162 [arXiv:1206.6278 [hep-ph]].
- [11] A. Arhrib, R. Benbrik, M. Chabab, G. Moultaqa, M. C. Peyranere, L. Rahili and J. Ramadan, Phys. Rev. D **84** (2011) 095005 [arXiv:1105.1925 [hep-ph]].
- [12] M. A. Schmidt, Phys. Rev. D **76** (2007) 073010 [Erratum-ibid. D **85** (2012) 099903] [arXiv:0705.3841 [hep-ph]]; W. Chao and H. Zhang, Phys. Rev. D **75** (2007) 033003 [hep-ph/0611323].
- [13] L. Lavoura and L. -F. Li, Phys. Rev. D **49** (1994) 1409 [hep-ph/9309262].
- [14] M. Baak, M. Goebel, J. Haller, A. Hoecker, D. Kennedy, R. Kogler, K. Moenig and M. Schott *et al.*, arXiv:1209.2716 [hep-ph].